Title	Remedial injected harmonic current operation of redundant flux-switching permanent magnet motor drives
Author(s)	Zhao, W; Cheng, M; Chau, KT; Cao, R; Ji, J
Citation	IEEE Transactions on Industrial Electronics, 2013, v. 60 n. 1, p. pp. 151-159
Issued Date	2013
URL	http://hdl.handle.net/10722/189039
Rights	IEEE Transactions on Industrial Electronics. Copyright © IEEE.

Remedial Injected-Harmonic-Current Operation of Redundant Flux-Switching Permanent-Magnet Motor Drives

Wenxiang Zhao, *Member, IEEE*, Ming Cheng, *Senior Member, IEEE*, K. T. Chau, *Senior Member, IEEE*, Ruiwu Cao, *Student Member, IEEE*, and Jinghua Ji

***Abstract*—Redundant flux-switching permanent-magnet (R-FSPM) motors are a new class of brushless machines having magnets in the stator, offering high power density, simple and robust rotor structure, and good thermal dissipation conditions. This paper proposes a new control strategy for fault-tolerant operation of the R-FSPM motor drive considering the capability limitation of the power converter. The key is to operate the R-FSPM motor in the remedial mode by injecting harmonic currents, the so-called remedial injected-harmonic-current (RIHC) operation mode. Moreover, the motor losses at the existing and the proposed remedial operations are compared for evaluation. Both cosimulation and experimental results are presented, confirming that the proposed RIHC operation can offer good steady-state and dynamic performances while reducing the motor losses and the capability requirements of the power converter during fault.**

***Index Terms*—Converter capability, fault-tolerant motors, loss, permanent-magnet (PM) motors, torque ripple.**

I. Introduction

With THE requirements for reducing emissions and improving fuel economy, electric vehicles (EVs) have attracted more and more attentions [1]. High reliability is an essential requirement for electric propulsion of EVs, where any types of fault would lead to disastrous effects on life safety [2]. Hence, continual operation of motor drives has been a growing demand [3].

In recent years, the development of fault-tolerant motor drives has received great attention, focusing on the switched reluctance (SR) motor and the conventional permanent-magnet (PM) brushless motor. SR motors have simple rotor construction and mechanical robustness, suitable for high-speed and high-reliability applications. Moreover, due to their decoupling phases, SR motors inherently possess the fault-tolerant characteristic [4]. By employing the redundant winding in the conventional SR machine topology, a new dual-channel SR machine was proposed for high-reliability operation of critical applications [5]. In [6], a new five-phase fault-tolerant SR motor drive with integrated and distributed inverter was developed for railway traction applications. On the other hand, PM brushless motors are emerging as a promising candidate for high-power-density and high-efficiency applications compared with SR motors [2]. A number of PM motors and control strategies with different degrees of fault-tolerant capability have appeared in the literature [3]. By employing an arrangement of alternately wound teeth in the stator, a new class of fractional-slot concentrated-winding fault-tolerant PM machines, termed as rotor-PM machines, was proposed for fault-tolerant operation [7], [8]. To operate the rotor-PM motor at flux weakening mode, a new control strategy was proposed in [9]. In addition, multiphase PM motors have received many attentions for fault-tolerant operation. In [10] and [11], the postfault current control strategies of a five-phase rotor-PM motor were proposed. The proposed control guarantees safe drive operation considering the third-harmonic components of the back electromotive forces (back EMFs).

However, since PMs are located in the rotor, these conventional rotor-PM brushless machines suffer from weak mechanical structure and difficulty in PM cooling. Thus, how to incorporate the merits of both high reliability and high power density has attracted more and more attentions. To retain the advantages of both SR and rotor-PM machines, a new class of brushless motors having magnets in the stator, termed as stator-PM motors, has been introduced [12]. Extensive research work has been performed to analyze this class of machines, showing that stator-PM motors incorporate the merits of high power density, short winding terminals, robust structure, and free from the thermal problem on PMs [13]. Recent work has shown that the doubly salient PM (DSPM) motor can inherently offer fault tolerance [14]. In [15], the remedial brushless ac (BLAC) mode has been proposed for fault-tolerant operation in a DSPM motor drive. However, it has been identified that the flux-switching PM (FSPM) motor has significantly higher power density than the DSPM one [16]–[18]. By introducing

Manuscript received July 26, 2011; revised October 30, 2011; accepted January 7, 2012. Date of publication January 26, 2012; date of current version September 6, 2012. This work was supported in part by the National Natural Science Foundation of China through grants under Projects 60974060, 50907031, and 51007031, by the Aeronautical Science Foundation of China under Project 20100769004, by the Priority Academic Program Development of Jiangsu Higher Education Institutions, and by the Professional Research Foundation for Advanced Talents of Jiangsu University, China, under Project 10JDG089.

W. Zhao and J. Ji are with the School of Electrical and Information Engineering, Jiangsu University, Zhenjiang 212013, China (e-mail: zwx@ujs.edu.cn; jjh@ujs.edu.cn).

M. Cheng and R. Cao are with the School of Electrical Engineering, Southeast University, Nanjing 210096, China (e-mail: mcheng@seu.edu.cn; ruiwucao@gmail.com).

K. T. Chau is with the Department of Electrical and Electronic Engineering, The University of Hong Kong, Hong Kong (e-mail: ktchau@eee.hku.hk).

Color versions of one or more of the figures in this paper are available online at http://ieeexplore.ieee.org.

Digital Object Identifier 10.1109/TIE.2012.2186107

the fault-tolerant concept into the FSPM machine, a new FSPM motor with redundant structure, termed as the redundant FSPM (R-FSPM) motor, has been proposed [19]. Differing from the conventional dual PM machines [20]–[22], the R-FSPM motor cannot be operated as two 3-phase machines because its back EMF contains harmonic components. Also, a compensating strategy, namely, setting $\sqrt{3}$ times the current amplitudes in two of the five remaining healthy coils, has been proposed to supplement the average torque and offset the harmonic torque under the open-circuit fault. However, since the current amplitudes of the remaining healthy coils are highly unequal, the power converter capability imposes the limiting factors to the remedial operation.

The purpose of this paper is to propose a new fault-tolerant operating strategy for the R-FSPM motor drives. The proposed operation differs from the existing one that it can decrease the current amplitude, hence requiring a lower converter capability than the reported solution in [19]. The key is to operate the R-FSPM motor in the remedial mode by injecting harmonic currents, the so-called remedial injected-harmonic-current (RIHC) operation mode. In Section II, the 12/10-pole R-FSPM motor will be briefly described and analyzed. Then, in Section III, in order to minimize the current amplitudes in the stator windings, proper harmonic currents for no-control generated-torque-ripple operation will be discussed, hence deducing the RIHC operation. Moreover, in Section IV, the performance of the proposed R-FSPM motor drive at the normal and the proposed RIHC operations will be assessed by using the cosimulation technique. Also, the motor losses at the existing and the proposed remedial operations will be compared. Furthermore, in Section V, experimental results will be used to verify the proposed RIHC operation of the motor drive. Finally, the conclusions will be drawn in Section VI.

II. Topology and Features

Fig. 1 shows the structure of the 12/10-pole R-FSPM motor, which has 12 salient poles in the stator, 10 salient poles in the rotor, 6 coil windings in the stator, and 10 PMs in the stator. In the proposed 12/10 R-FSPM motor, the two opposing windings on poles form one coil, such as coils A1 and A2. Notice that, in the conventional 12/10 FSPM motor, coils A1 and A2 are in series to build up phase A.

The R-FSPM motor actually incorporates the merits as follows.

1) Similar to the DSPM motors having PMs in the stator, the R-FSPM motor incorporates the merits of the SR motor and the rotor-PM motor, thus offering robust rotor structure, good cooling conditions for magnets, and high power density.
2) Similar to the fault-tolerant motors, the R-FSPM motor possesses the features of redundant winding structure and independent phases in electric and magnetic circuits, thus providing the possibility of fault-tolerant operation.
3) Different from the DSPM motors, the R-FSPM motor has bipolar winding PM flux linkage, thus achieving higher torque density and higher power density.

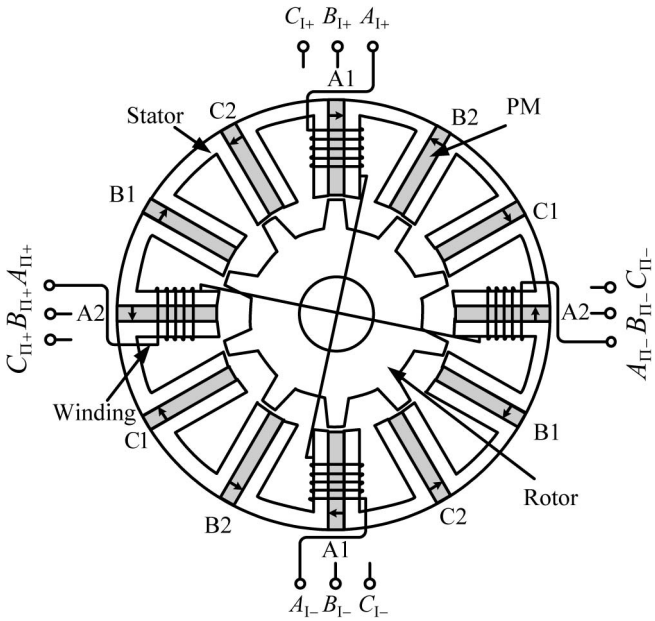

Fig. 1. Cross section of 12/10-pole R-FSPM motor.

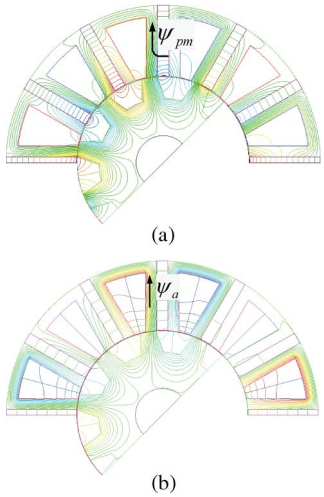

Fig. 2. Magnetic field distributions. (a) PMs only. (b) Armature current only.

4) Different from most of the conventional PM brushless motors, the R-FSPM motor solves the problem of the influence of armature reaction field on the working point of PMs under the short-circuit fault because its windings and magnets are magnetically in parallel, as shown in Fig. 2, hence inherently suitable for high-reliability applications.

Fig. 3 shows the predicted coil and phase back EMFs at no load as compared with the measured ones. It should be noted that the measured back EMFs are not very identical with the predicted ones due to the end effect of the stator-PM machines [23]. It can be seen that each coil back EMF has rich harmonic components, whereas the corresponding phase back EMF is close to sinusoidal in shape. This is due to the compensation of harmonic components in the coils. Moreover, harmonic analysis is performed for the coil and the phase back EMFs as listed in Table I, in which the harmonic magnitude is expressed as the percentage of the fundamental amplitude. Obviously, the second harmonic is the main harmonic component, while the

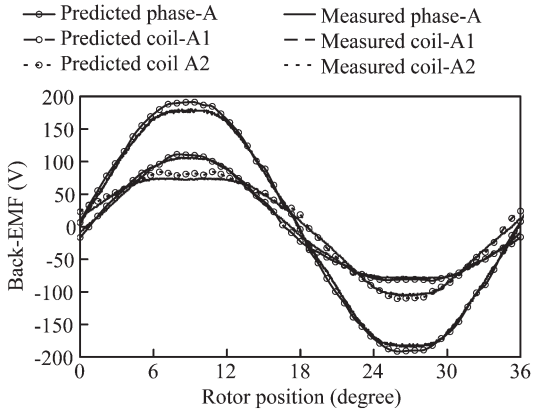

Fig. 3. Predicted and measured back-EMF waveforms at no load.

TABLE I
HARMONIC ANALYSIS OF BACK EMFS

Harmonic magnitude (%)	Coil-A1	Coil-A2	Phase-A
2nd harmonic	14.79	14.74	0.68
3rd harmonic	0.58	0.83	0.77
4th harmonic	1.88	1.77	0.25
5th harmonic	0.78	0.98	0.83
Total harmonic distortion	15.17	15.11	1.78

third and the higher harmonics can be neglected. Consequently, by considering only the fundamental and second-harmonic components, the back EMFs of the R-FSPM machine can be expressed as

$$\begin{cases} e_{a1} = E_1 \sin(\omega_e t) + E_2 \sin(2\omega_e t + \varphi) \\ e_{b1} = E_1 \sin(\omega_e t + 2\pi/3) + E_2 \sin(2\omega_e t + \varphi - 2\pi/3) \\ e_{c1} = E_1 \sin(\omega_e t - 2\pi/3) + E_2 \sin(2\omega_e t + \varphi + 2\pi/3) \\ e_{a2} = E_1 \sin(\omega_e t) - E_2 \sin(2\omega_e t + \varphi) \\ e_{b2} = E_1 \sin(\omega_e t + 2\pi/3) - E_2 \sin(2\omega_e t + \varphi - 2\pi/3) \\ e_{c2} = E_1 \sin(\omega_e t - 2\pi/3) - E_2 \sin(2\omega_e t + \varphi + 2\pi/3) \end{cases} \tag{1}$$

where ω_e is the frequency of the fundamental component (the rotor electrical speed), φ is the second-harmonic angle relative to the fundamental phase, and E_1 and E_2 are the amplitudes of the fundamental and the second-harmonic back EMFs, respectively.

III. RIHC OPERATION

The proposed strategy in this section involves two techniques. First, after the occurrence of an open-circuit fault, the remedial operation can maintain the torque output as the normal operation. Second, at the remedial operation, the current amplitudes of the remaining coils are controlled at the same value in order to reduce the capability requirements of the converter. The fundamental and the second-harmonic current components are used to excite the healthy coils in order to eliminate harmonic torque generated by unbalanced faulty operation. Consequently, the proposed remedial operation calculates the excitation currents for the healthy phases to produce the desired output torque with minimum torque ripple and reduced requirements of the converter capability.

A. Normal Condition

Under the normal condition, the R-FSPM motor operates in the BLAC mode, in which all coils are in work. The motor currents are given as

$$\begin{cases} i_{a1} = I_m \sin(\omega_e t) \\ i_{b1} = I_m \sin(\omega_e t + 2\pi/3) \\ i_{c1} = I_m \sin(\omega_e t - 2\pi/3) \\ i_{a2} = I_m \sin(\omega_e t) \\ i_{b2} = I_m \sin(\omega_e t + 2\pi/3) \\ i_{c2} = I_m \sin(\omega_e t - 2\pi/3) \end{cases} \tag{2}$$

where I_m is the amplitude of the sinusoidal current.

For the R-FSPM motors, the electromagnetic torque predominantly is resulted from the PM torque component since the reluctance torque component is negligible. Thus, the electromagnetic torque at normal operation can be calculated as

$$\begin{aligned} T_{en} &= T_1 + T_2 \\ &= (1/\omega_m) \sum_{p=a}^{c} (e_{p1} \cdot i_{p1} + e_{p2} \cdot i_{p2}) \\ &= \left[3E_1 I_m - 0.45 E_1 I_m \cos(3\omega t + 2\pi/5)\right] / 2\omega_m \\ &\quad + \left[3E_1 I_m + 0.45 E_1 I_m \cos(3\omega t + 2\pi/5)\right] / 2\omega_m \\ &= 3E_1 I_m / \omega_m \end{aligned} \tag{3}$$

where ω_m is the rotor mechanical speed and T_1 and T_2 are the electromagnetic torque produced by coils A1, B1, and C1 and the electromagnetic torque produced by coils A2, B2, and C2, respectively. It can be deduced from (3) that, when it operates in the normal BLAC mode, the R-FSPM motor has a constant electromagnetic torque because the harmonic torque counteracts each other.

B. Faulty Condition

When the R-FSPM motor drive is under fault, the faulty coil can be shut off, and the healthy coils can continue their operation. Thus, proper fault detectors need to be employed. It should be noted that the fault detection technique for motor drives has been reported in many literatures [24]–[26], and this paper focuses on the development of the remedial control operation.

For the reduced capability requirements and the no-control generated-torque-ripple operation, the RIHC control strategy of the R-FSPM motor is proposed. The key is to operate the R-FSPM motor with the proper injected harmonic currents to compensate for harmonic back-EMF components, thus keeping the same current amplitudes in the healthy coils. In the following analysis, a failure in coil A1 is considered as an example.

In the RIHC operation mode, the remedial currents of the healthy coils are expressed as

$$\begin{cases} i'_{a1} = 0 \\ i'_{b1} = I_1 \sin(\omega_e t + 5\pi/6) + I_2 \sin(2\omega_e t + \alpha) \\ i'_{c1} = I_1 \sin(\omega_e t - 5\pi/6) + I_2 \sin(2\omega_e t + \beta) \\ i_{a2} = I_1 \sin(\omega_e t) \\ i_{b2} = I_1 \sin(\omega_e t + 2\pi/3) \\ i'_{c2} = I_1 \sin(\omega_e t - 2\pi/3) \end{cases} \tag{4}$$

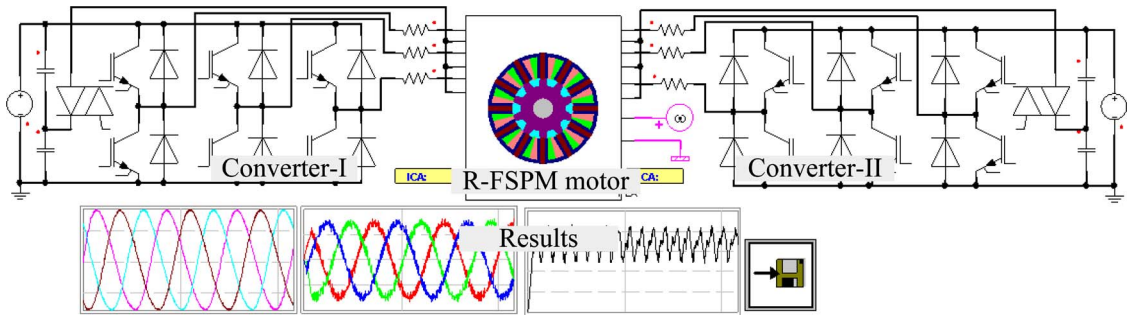

Fig. 4. Cosimulation model of R-FSPM motor drive.

where I_1 is the amplitude of the fundamental currents in the remaining phases, I_2 is the amplitude of the second-harmonic currents, and α and β are the harmonic angles of the second-harmonic currents relative to the fundamental component.

The electromagnetic torque T_2 can be calculated as

$$\begin{aligned} T_2 &= (1/\omega_m)\cdot(e_{a2}\cdot i_{a2}+e_{b2}\cdot i_{b2}+e_{c2}\cdot i_{c2}) \\ &= (1/\omega_m)\cdot[3E_1I_1/2+3E_2I_1\cos(3\omega_e t+\varphi)/2]. \end{aligned} \tag{5}$$

Meanwhile, the electromagnetic torque T_1 can be calculated as

$$\begin{aligned} T_1 =& (1/\omega_m)\cdot(0+e_{b1}\cdot i_{b1}+e_{c1}\cdot i_{c1}) \\ =& (1/\omega_m)\left\{\frac{\sqrt{3}}{2}E_1I_1-\frac{\sqrt{3}}{2}E_2I_1\cos(3\omega t+\varphi)\right. \\ &+E_1I_2\left[\cos\left(\omega t+\frac{\alpha+\beta}{2}\right)\cdot\cos\left(\frac{\alpha-\beta}{2}-2\pi/3\right)\right. \\ &\left.-\cos\left(3\omega t+\frac{\alpha+\beta}{2}\right)\right. \\ &\left.\cdot\cos\left(\frac{\alpha-\beta}{2}+2\pi/3\right)\right] \\ &+E_2I_2\left[\cos\left(\varphi-\frac{\alpha+\beta}{2}\right)\cdot\cos\left(-2\pi/3-\frac{\alpha-\beta}{2}\right)\right. \\ &\left.-\cos\left(4\omega t+\varphi+\frac{\alpha+\beta}{2}\right)\right. \\ &\left.\left.\cdot\cos\left(\frac{\alpha-\beta}{2}-2\pi/3\right)\right]\right\}. \end{aligned} \tag{6}$$

For no-control generated-torque-ripple operation, there are two constraints, as given by

$$\begin{cases} \cos\left(\frac{\alpha-\beta}{2}-2\pi/3\right)=0 \\ \frac{\alpha+\beta}{2}=\varphi. \end{cases} \tag{7}$$

This leads to

$$\begin{cases} \alpha=\varphi+\pi/6 \\ \beta=\varphi-\pi/6. \end{cases} \tag{8}$$

Thus, by substituting (8) into (6), the electromagnetic torque T_1 can be calculated as

$$\begin{aligned} T_1 = (1/\omega_m)\cdot\left[\frac{\sqrt{3}}{2}(E_1I_1-E_2I_2)-\frac{\sqrt{3}}{2}(E_2I_1-E_1I_2)\right. \\ \left.\cdot\cos(3\omega t+\varphi)\right]. \end{aligned} \tag{9}$$

The same torque before and after the fault can be kept invariant by substituting (5) and (9) into (3), yielding

$$\begin{cases} \frac{3}{2}E_2I_1=\frac{\sqrt{3}}{2}(E_2I_1-E_1I_2) \\ \frac{3}{2}E_1I_1+\frac{\sqrt{3}}{2}(E_1I_1-E_2I_2)=3E_1I_m. \end{cases} \tag{10}$$

Thus, the amplitudes of remedial currents can be expressed in terms of E_1, E_2, and I_m

$$\begin{cases} I_1=\frac{6I_mE_1^2}{(3+\sqrt{3})E_1^2+(3-\sqrt{3})E_2^2} \\ I_2=\frac{6(1-\sqrt{3})I_mE_1E_2}{(3+\sqrt{3})E_1^2+(3-\sqrt{3})E_2^2}. \end{cases} \tag{11}$$

Also, the harmonic analysis of the back EMFs deduces

$$\begin{cases} \varphi=5\pi/12 \\ E_2=0.15E_1. \end{cases} \tag{12}$$

Thus, by using (4), (11), and (12), the proposed RIHC operation after the loss of coil A1 is achieved, as given by

$$\begin{cases} i'_{a1}=0 \\ i'_{b1}=1.27I_m\left[\sin(\omega t+5\pi/6)-0.12\sin(2\omega t+7\pi/12)\right] \\ i'_{c1}=1.27I_m\left[\sin(\omega t-5\pi/6)-0.12\sin(2\omega t+\pi/4)\right] \\ i_{a2}=1.27I_m\sin(\omega t) \\ i_{b2}=1.27I_m\sin(\omega t+2\pi/3) \\ i'_{c2}=1.27I_m\sin(\omega t-2\pi/3). \end{cases} \tag{13}$$

Of course, a similar operation can be applied to the loss of other coils. Meanwhile, it can be confirmed that, by injecting the second-harmonic currents, the R-FSPM motor can operate in the RIHC mode, in which the restructured fault-tolerant torque can effectively replace the normal torque.

IV. Simulation

This work employs the cosimulation modeling method of the magnetic circuit and the electric circuit to predict the performance of the proposed R-FSPM motor drive, in which the system level simulation is provided [14]. Fig. 4 shows the developed transient cosimulation model of the R-FSPM motor drive. The R-FSPM motor is driven by two independent sets of power electronic circuit and controller.

To assess the torque performance at the normal and the proposed remedial operations, a torque ripple factor is defined as follows:

$$K_T=\frac{T_{\max}-T_{\min}}{T_{\text{av}}}\times 100\% \tag{14}$$

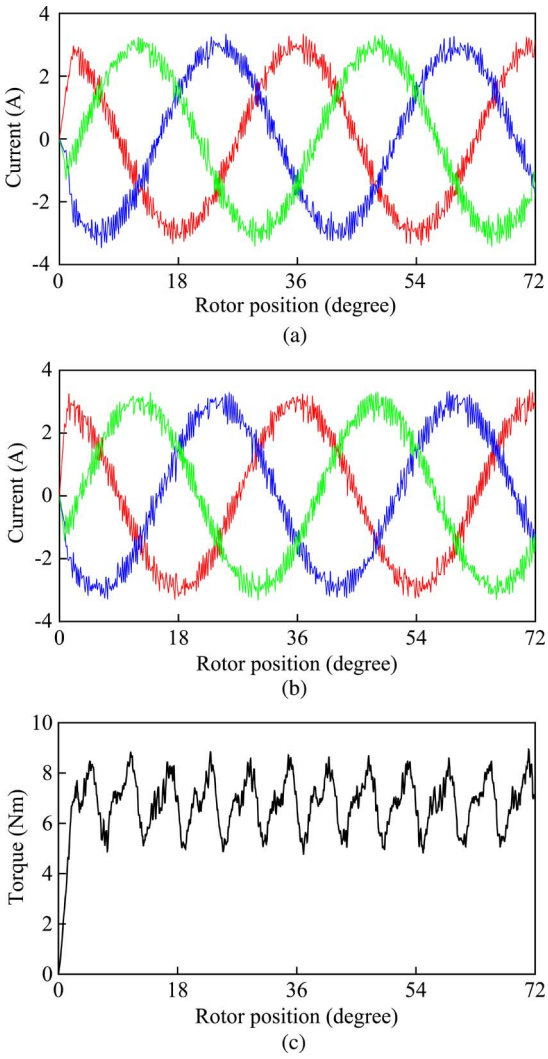

Fig. 5. Waveforms at normal operation. (a) Currents of coils A1, B1, and C1. (b) Currents of coils A2, B2, and C2. (c) Torque.

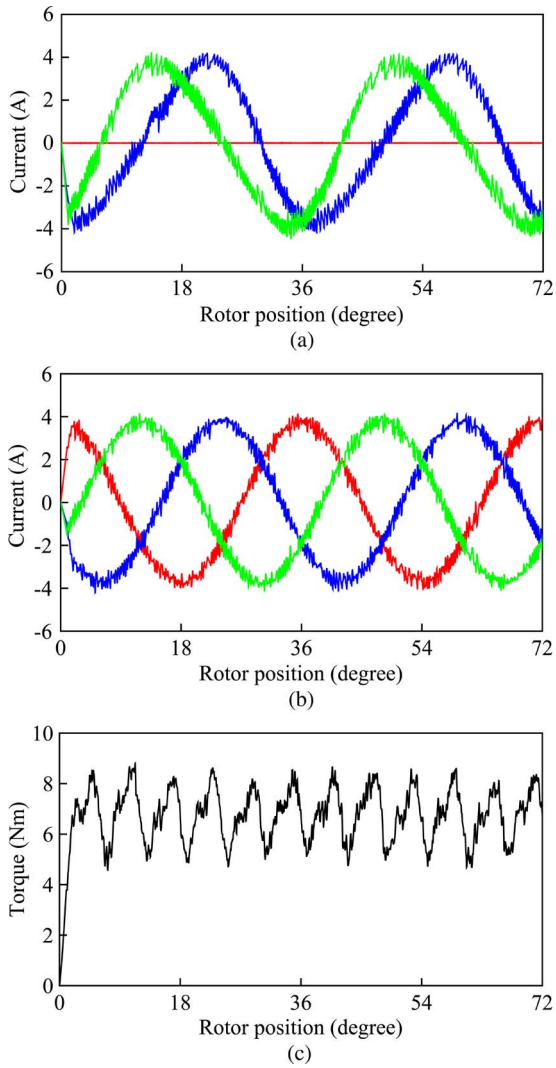

Fig. 6. Waveforms at the proposed RIHC operation. (a) Currents of coils A1, B1, and C1. (b) Currents of coils A2, B2, and C2. (c) Torque.

where $T_{\max}$, $T_{\min}$, and T_{av} are the maximum value, the minimum value, and the average value of the output torque, respectively.

During normal operation, the R-FSPM motor drive operates in the BLAC mode. By using (2), the motor current and torque waveforms are cosimulated, as shown in Fig. 5. It can be seen that the current waveform is sinusoidal and the corresponding T_{av} and K_T of the motor drive are 6.6 N · m and 59.3%, respectively. It should be noted that the torque ripple is caused by the cogging torque in the R-FSPM machine [27].

In the event of open-circuit fault, one coil is lost, and the healthy five coils continue their operation. Then, the proposed RIHC operation is activated by using (13). As shown in Fig. 6, both of the coil-B1 and coil-C1 currents are constituted by the fundamental and second-harmonic components, while the current waveforms of coils A2, B2, and C2 are sinusoidal. The corresponding T_{av} and K_T are 6.2 N · m and 63.3%, respectively. By comparing the values at normal and remedial operations, it can be found that their torque performances are practically the same. The slight discrepancies are due to the neglected third-harmonic and higher harmonic components of back EMFs. These cosimulated results verify that the proposed RIHC operation can maintain the same torque under the open-circuit fault.

It is well known that the loss results in temperature rise, which is a critical issue for high-reliability operation. Thus, the losses of the existing remedial operation in [19] and the proposed remedial operation in this paper are compared for evaluation. At the existing remedial operation, during the loss of coil A1, the current amplitudes of coils B1 and C1 are regulated to $\sqrt{3}$ times the normal values before fault, and the phase angles of coils B1 and C1 are correspondingly changed. Meanwhile, the currents of coils A2, B2, and C2 are kept invariant.

First, the copper loss can be calculated by a straightforward way, as given by

$$P_C = \sum_{p=A}^{C} \left(I_{p1}^2 + I_{p2}^2\right) R_p \tag{15}$$

where R_p and I_p ($p = A$, B, and C) are the motor winding resistance and rms current, respectively. So, as compared with the

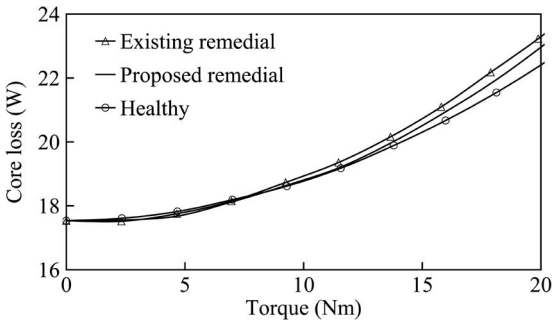

Fig. 7. Iron losses at existing remedial, proposed remedial, and healthy operations.

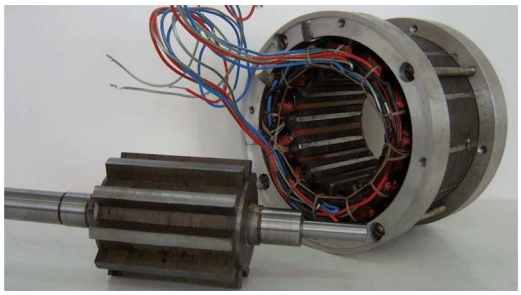

Fig. 8. R-FSPM prototype machine.

existing one, the proposed remedial operation in (13) reduces nearly 10% copper loss.

Second, a time-stepping finite-element method is employed to predict the core losses in both remedial operations. Since their current amplitudes are different, the torque–iron loss characteristics are investigated, as shown in Fig. 7. It can be seen that the iron loss at the proposed remedial operation is slightly lower than that of the existing remedial operation, even in the presence of injected harmonic currents. This is due to the fact that the existing remedial operation employs higher current amplitudes. The associated armature reaction field is, therefore, stronger and results in a greater iron loss.

Finally, by comprehensively evaluating the total motor losses, including the copper loss and the iron loss, it can be confirmed that the proposed remedial operation has lower losses than the existing one.

In addition, it should be noted that, although the proposed remedial operation has higher efficiency than the existing one, it is still inferior to the healthy operation. This is due to the unbalanced operation under the fault condition. It can be calculated by using (15) that the proposed remedial operation has 33% higher copper loss than the healthy operation. Also, it can be known from Fig. 7 that the proposed remedial operation has higher core loss than the healthy operation.

V. Experimental Validation

To further verify the theoretical analysis, a 12/10-pole R-FSPM motor is designed and prototyped, as shown in Fig. 8. Based on the digital signal processing TMS320F2812 controller, an experimental test-rig bed has been built. It is composed of an R-FSPM motor supplied by two independent IPM-based converters, a separately excited dc generator used as the variable load, and a transient torque transducer mounted between the R-FSPM motor and the dc generator to measure the torque of the proposed motor drive. In the experiment, the currents of the machine are sensed by six Hall-effect current sensors, and an optical encoder with an accuracy of 2048 counts per revolution is used to obtain position information.

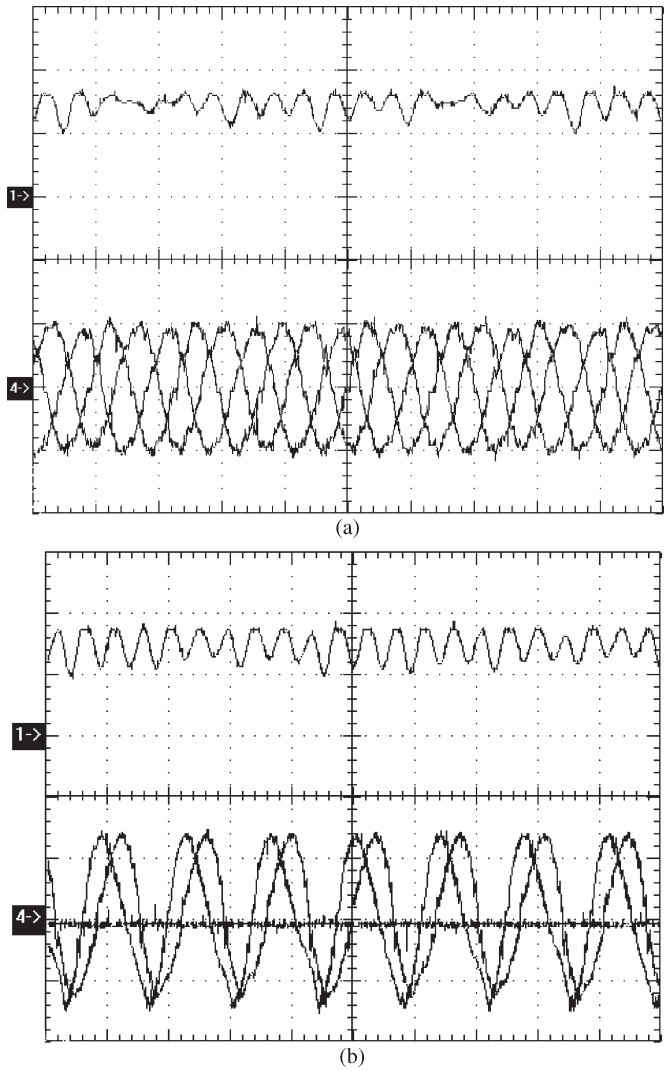

Fig. 9. Measured (upper trace) torque waveform and (lower traces) current waveforms (5 ms/div, 4 N · m/div, and 3 A/div). (a) Normal operation. (b) RIHC operation.

First, the steady-state performance of the proposed R-FSPM motor drive is assessed. Fig. 9 compares the steady-state torque and current waveforms under the normal and the proposed RIHC operations. As expected, these current waveforms agree with the cosimulated ones shown in Figs. 5 and 6, verifying that the proposed remedial operation can maintain the torque performance. Fig. 10 compares the fault-tolerant current waveforms of coils B1, C1, B2, and C2 during the loss of coil A1, showing that the currents of coils B1 and C1 are slightly distorted. Also, it can be noted that the peak values of these currents are same.

It should be noted that the measured torque waveforms have a significant discrepancy with those cosimulated ones shown in Figs. 5 and 6. This discrepancy is due to the fact that the predicted torque waveforms take into account the cogging

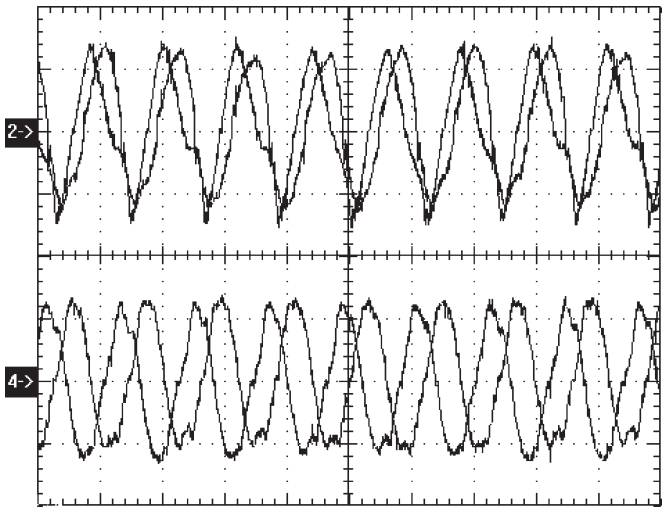

Fig. 10. Measured current waveforms of (upper traces) coils B1 and C1 and (lower traces) coils B2 and C2 at RIHC operation (5 ms/div; 3 A/div).

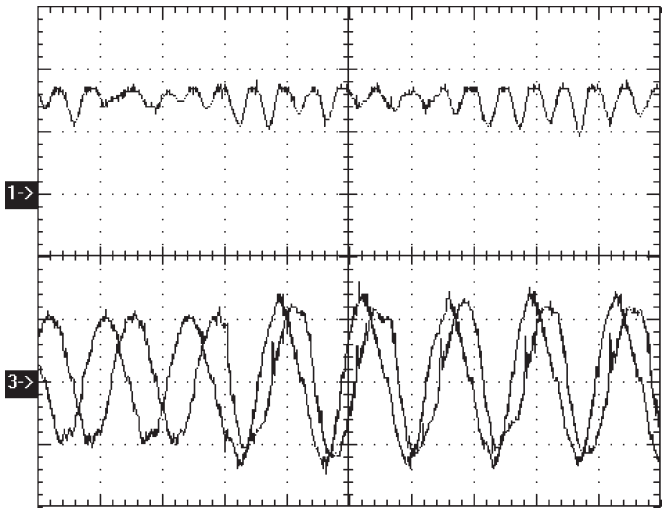

Fig. 11. Measured (upper trace) torque waveform and (lower traces) current waveforms before and after the fault (10 ms/div, 3 N · m/div, and 3 A/div).

torque ripple only, whereas the measured torque waveforms consist of all torque ripples, such as the operating, practical, and manufacturing torque ripples. Notice that both the practical and manufacturing torque ripples are very difficult to be modeled mathematically. Nevertheless, for the normal and remedial operations, the measured torque performances (average torque and torque ripple) are equivalent, verifying the effectiveness of the proposed remedial operation.

Second, the dynamic performance of the proposed R-FSPM motor drive is evaluated. Fig. 11 shows the responses of torque and current before and after the remedial operation. It can be found that the motor drive can online switch to the fault-tolerant mode.

Third, the self-starting capability at the proposed RIHC operation is particularly assessed, which is essential for EVs desiring frequent start–stop. Fig. 12 shows the start-up current responses at the proposed RIHC operation (the load applied at start-up is 5.7 N · m), confirming that the R-FSPM motor drive can successfully perform self-starting during the loss of one coil.

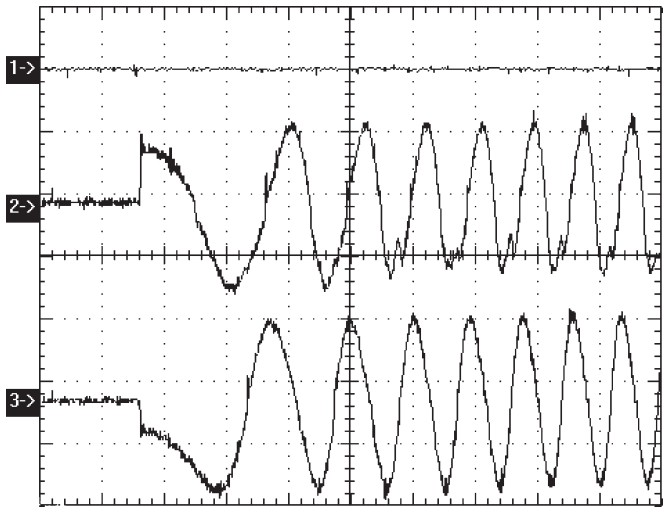

Fig. 12. Measured current responses at start-up (25 ms/div; 3 A/div).

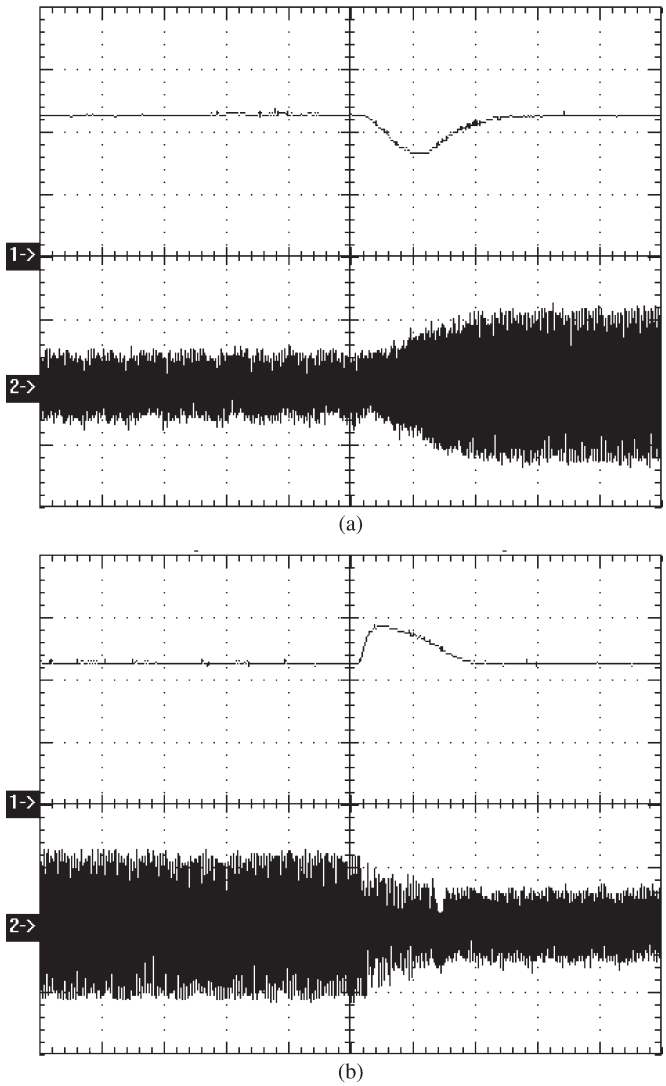

Fig. 13. Measured (upper trace) speed response and (lower trace) current response at load change (0.5 s/div, 200 r/min/div, and 6 A/div). (a) Load increase. (b) Load decrease.

Finally, the dynamic load test of the developed motor drive at the proposed RIHC operation is performed. Fig. 13 shows the dynamic responses of speed and current under sudden changes

of load torque when the motor operates in the fault-tolerant mode (from 2.3 to 5.7 N · m and then back to 2.3 N · m). It can be found that the transient changes in speed are quite small, while the speed regulation is very good.

VI. Conclusion

In this paper, the RIHC control strategy has been newly proposed and implemented for fault-tolerant operation of the R-FSPM motor drive. By injecting second-harmonic currents, the RIHC operation is proposed to reduce the capability requirements of power converter and provide no-control generated-torque-ripple operation. It also reveals that the RIHC operation can offer good steady-state and dynamic performances. The validity of the proposed remedial control strategies has been verified by cosimulation and experimental results, showing that the proposed approach can reduce the capability requirements of the converter, lower the motor losses, maintain the torque performance, retain the self-starting capability, and offer good speed regulation with load changes during the loss of one coil. The proposed remedial operation is particularly important to enable continued operation for many practical applications such as EVs.

References

[1] C. C. Chan, "The state of the art of electric, hybrid, and fuel cell vehicles," *Proc. IEEE*, vol. 95, no. 4, pp. 704–718, Apr. 2007.

[2] K. T. Chau, C. C. Chan, and C. Liu, "Overview of permanent magnet brushless drives for electric and hybrid electric vehicles," *IEEE Trans. Ind. Electron.*, vol. 55, no. 6, pp. 2246–2257, Jun. 2008.

[3] A. M. El-Refaie, "Fault-tolerant permanent magnet machines: A review," *IET Elect. Power Appl.*, vol. 5, no. 1, pp. 59–74, Jan. 2011.

[4] C. M. Stephens, "Fault detection and management system for fault-tolerant switched reluctance motor drives," *IEEE Trans. Ind. Appl.*, vol. 27, no. 6, pp. 1098–1102, Nov./Dec. 1991.

[5] W. Ding and D. Liang, "Comparison of transient and steady-state performances analysis for a dual-channel switched reluctance machine operation under different modes," *IET Elect. Power Appl.*, vol. 4, no. 8, pp. 603–617, Sep. 2010.

[6] M. D. Hennen, M. Niessen, C. Heyers, H. J. Brauer, and R. W. De Doncker, "Development and control of an integrated and distributed inverter for a fault tolerant five-phase switched reluctance traction drive," *IEEE Trans. Power Electron.*, vol. 27, no. 2, pp. 547–554, Feb. 2012.

[7] A. G. Jack, B. C. Mecrow, and J. Haylock, "A comparative study of permanent magnet and switched reluctance motors for high-performance fault-tolerant applications," *IEEE Trans. Ind. Appl.*, vol. 32, no. 4, pp. 889–895, Jul./Aug. 1996.

[8] A. M. EL-Refaie, "Fractional-slot concentrated-windings synchronous permanent magnet machines: Opportunities and challenges," *IEEE Trans. Ind. Electron.*, vol. 57, no. 1, pp. 107–121, Jan. 2010.

[9] Z. Sun, J. Wang, G. Jewell, and D. Howe, "Enhanced optimal torque control of fault-tolerant permanent magnet machines under flux weakening operations," *IEEE Trans. Ind. Electron.*, vol. 57, no. 1, pp. 344–353, Jan. 2010.

[10] L. Parsa and H. A. Toliyat, "Fault-tolerant interior-permanent-magnet machines for hybrid electric vehicle applications," *IEEE Trans. Veh. Technol.*, vol. 56, no. 4, pp. 1546–1552, Jul. 2007.

[11] S. Dwari and L. Parsa, "Fault-tolerant control of five-phase permanent magnet motors with trapezoidal back-EMF," *IEEE Trans. Ind. Electron.*, vol. 58, no. 2, pp. 476–485, Feb. 2011.

[12] M. Cheng, W. Hua, J. Zhang, and W. Zhao, "Overview of stator-permanent magnet brushless machines," *IEEE Trans. Ind. Electron.*, vol. 58, no. 11, pp. 5087–5101, Nov. 2011.

[13] A. S. Thomas, Z. Q. Zhu, and G. W. Jewell, "Comparison of flux switching and surface mounted permanent magnet generators for high-speed applications," *IET Elect. Syst. Transp.*, vol. 1, no. 3, pp. 111–116, Sep. 2011.

[14] W. Zhao, M. Cheng, X. Zhu, W. Hua, and X. Kong, "Analysis of fault-tolerant performance of a doubly salient permanent-magnet motor drive using transient cosimulation method," *IEEE Trans. Ind. Electron.*, vol. 55, no. 4, pp. 1739–1748, Apr. 2008.

[15] W. Zhao, K. T. Chau, M. Cheng, J. Ji, and X. Zhu, "Remedial brushless AC operation of fault-tolerant doubly-salient permanent-magnet motor drives," *IEEE Trans. Ind. Electron.*, vol. 57, no. 6, pp. 2134–2141, Jun. 2010.

[16] J. Zhang, M. Chenga, Z. Chen, and W. Hua, "Comparison of stator-mounted permanent-magnet machines based on a general power equation," *IEEE Trans. Energy Convers.*, vol. 24, no. 4, pp. 826–834, Dec. 2009.

[17] Z. Q. Zhu and J. T. Chen, "Advanced flux-switching permanent magnet brushless machines," *IEEE Trans. Magn.*, vol. 46, no. 6, pp. 1447–1453, Jun. 2010.

[18] T. Raminosoa, C. Gerada, and M. Galea, "Design considerations for a fault-tolerant flux-switching permanent-magnet machine," *IEEE Trans. Ind. Electron.*, vol. 58, no. 7, pp. 2818–2825, Jul. 2011.

[19] W. Zhao, M. Cheng, W. Hua, H. Jia, and R. Cao, "Back-EMF harmonic analysis and fault-tolerant control of flux-switching permanent-magnet machine with redundancy," *IEEE Trans. Ind. Electron.*, vol. 58, no. 5, pp. 1926–1935, May 2011.

[20] W. U. N. Fernando, M. Barnes, and O. Marjanovic, "Direct drive permanent magnet generator fed AC–DC active rectification and control for more-electric aircraft engines," *IET Elect. Power Appl.*, vol. 5, no. 1, pp. 14–27, Jan. 2011.

[21] M. Barcaro, N. Bianchi, and F. Magnussen, "Faulty operations of a PM fractional-slot machine with a dual three-phase winding," *IEEE Trans. Ind. Electron.*, vol. 58, no. 9, pp. 3825–3832, Sep. 2011.

[22] F. Lin, P. Chou, C. Chen, and Y. Lin, "DSP-based cross-coupled synchronous control for dual linear motors via intelligent complementary sliding mode control," *IEEE Trans. Ind. Electron.*, vol. 59, no. 2, pp. 1061–1073, Feb. 2012.

[23] Z. Q. Zhu, Y. Pang, W. Hua, M. Cheng, and D. Howe, "Investigation of end effect in permanent magnet brushless machines having magnets on the stator," *J. Appl. Phys.*, vol. 99, no. 8, pp. 08R319-3-1–08R319-3-3, Apr. 2006.

[24] S. Nandi, H. A. Toliyat, and X. Li, "Condition monitoring and fault diagnosis of electrical motors—A review," *IEEE Trans. Energy Convers.*, vol. 20, no. 4, pp. 719–729, Dec. 2005.

[25] A. Gandhi, T. Corrigan, and L. Parsa, "Recent advances in modeling and online detection of stator interturn faults in electrical motors," *IEEE Trans. Ind. Electron.*, vol. 58, no. 5, pp. 1564–1575, May 2011.

[26] S. Khwan-on, L. de Lillo, L. Empringham, and P. Wheeler, "Fault-tolerant matrix converter motor drives with fault detection of open switch faults," *IEEE Trans. Ind. Electron.*, vol. 59, no. 1, pp. 257–268, Jan. 2012.

[27] W. Fei, P. C. K. Luk, J. Shen, B. Xia, and Y. Wang, "Permanent-magnet flux-switching integrated starter generator with different rotor configurations for cogging torque and torque ripple mitigations," *IEEE Trans. Ind. Appl.*, vol. 47, no. 3, pp. 1247–1256, May/Jun. 2011.

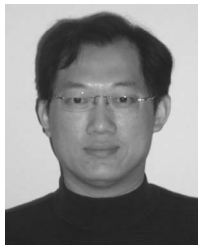

Wenxiang Zhao (M'08) was born in Jilin, China, in 1976. He received the B.Sc. and M.Sc. degrees in electrical engineering from Jiangsu University, Zhenjiang, China, in 1999 and 2003, respectively, and the Ph.D. degree in electrical engineering from Southeast University, Nanjing, China, in 2010.

Since 2003, he has been with Jiangsu University, where he is currently an Associate Professor in the School of Electrical Information Engineering. His areas of interest include electric machine design, modeling, fault analysis, and intelligent control.

Ming Cheng (M'01–SM'02) received the B.Sc. and M.Sc. degrees from the Department of Electrical Engineering, Southeast University, Nanjing, China, in 1982 and 1987, respectively, and the Ph.D. degree from the Department of Electrical and Electronic Engineering, The University of Hong Kong, Hong Kong, in 2001.

Since 1987, he has been with Southeast University, where he is currently a Professor in the School of Electrical Engineering and the Director of the Research Center for Wind Power Generation. From January to April 2011, he was a Visiting Professor in Wisconsin Electric Machine and Power Electronics Consortium, University of Wisconsin, Madison. His teaching and research interests include electrical machines, motor drives for electric vehicles, and renewable-energy generation. He has authored or coauthored over 250 technical papers and 4 books and is the holder of 45 patents in these areas.

Dr. Cheng is a Fellow of The Institution of Engineering and Technology. He has served as the Chair and an organizing committee member for many international conferences.

K. T. Chau (M'89–SM'04) received the B.Sc.(Eng.) (with first-class honors), M.Phil., and Ph.D. degrees in electrical and electronic engineering from The University of Hong Kong, Hong Kong, in 1988, 1991, and 1993, respectively.

He is currently a Full Professor with the Department of Electrical and Electronic Engineering, The University of Hong Kong, where he is also the Director of the International Research Center for Electric Vehicles. His teaching and research interests focus on three main areas: electric and hybrid vehicles, machine and drives, and clean energy. In these areas, he has published four books, seven book chapters, and over 180 refereed journal papers.

Dr. Chau is a fellow of The Institution of Engineering and Technology. He was the recipient of the Chang Jiang Chair Professor Award from the Ministry of Education of China in 2008, the Environmental Excellence in Transportation Award for Education, Training and Public Awareness from SAE International in 2006, the Award for Innovative Excellence in Teaching, Learning and Technology at the International Conference on College Teaching and Learning in 2005, and the University Teaching Fellow Award from The University of Hong Kong in 2004.

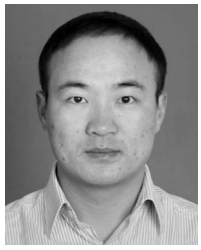

Ruiwu Cao (S'10) was born in Jiangsu, China, in 1980. He received the B.Sc. degree in electrical engineering from Yancheng Institute of Technology, Yancheng, China, in 2004 and the M.Sc. degree in electrical engineering from Southeast University, Nanjing, China, in 2007, where he is currently working toward the Ph.D. degree in electrical engineering.

From 2007 to 2009, he was a Hardware Electrical Engineer with Bosch and Siemens Household Electrical Appliances, Nanjing. In 2010, he was a joint Ph.D. student funded by China Scholarship Council with the College of Electrical and Computer Science, University of Michigan, Dearborn, where he worked on permanent-magnet motors. His areas of interests include design, analysis, and control of permanent-magnet linear machines.

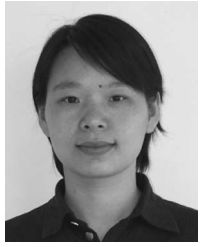

Jinghua Ji was born in Jiangsu, China, in 1977. She received the B.Sc., M.Sc., and Ph.D. degrees in electrical engineering from Jiangsu University, Zhenjiang, China, in 2000, 2003, and 2009, respectively.

Since 2000, she has been with the School of Electrical and Information Engineering, Jiangsu University, where she is currently an Associate Professor. Her areas of interest include motor design and electromagnetic field computation.